Kv1.2 Channels Promote Nonlinear Spiking Motoneurons for Powering Up Locomotion

Rémi Bos, Ronald M Harris-Warrick, Cécile Brocard, Liliia Demianenko, Marin Manuel, Daniel Zytnicki, Sergiy M Korogod, Frédéric Brocard

Article

Cell Reports

Kv1.2 Channels Promote Nonlinear Spiking Motoneurons for Powering Up Locomotion

Graphical Abstract

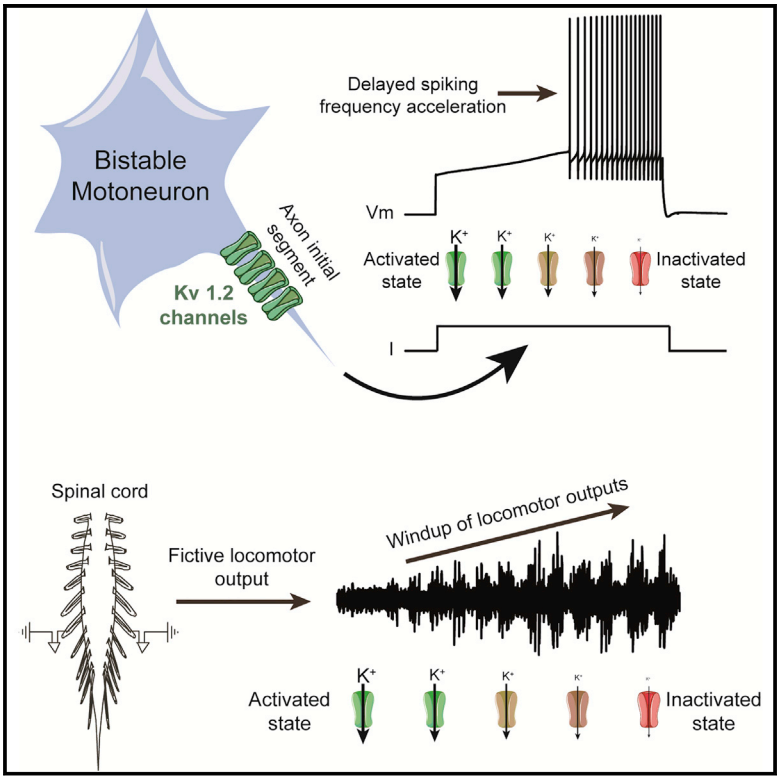

Highlights

- Neonatal and adult bistable motoneurons display delayed spike-frequency acceleration
- Delayed spike-frequency acceleration reflects slow inactivation of Kv1.2 channels
- Kv1.2 channels are highly expressed in axon initial segments of motoneurons
- Slow inactivation of Kv1.2 channels amplifies motor outputs upon locomotion onset

Authors

Rémi Bos, Ronald M. Harris-Warrick, Cécile Brocard, ..., Daniel Zytnicki, Sergiy M. Korogod, Frédéric Brocard

Correspondence

frederic.brocard@univ-amu.fr

In Brief

Bos et al. demonstrate that slow inactivation of Kv1.2 channels is critical in shaping nonlinear firing properties in mammalian spinal cord. It provides a potent gain control mechanism in spinal motoneurons and has a behavioral role in enhancing locomotor drive during the transition from immobility to steady-state locomotion.

Bos et al., 2018, Cell Reports 22, 3315–3327
March 20, 2018
https://doi.org/10.1016/j.celrep.2018.02.093

CellPress

Cell Reports
Article

Kv1.2 Channels Promote Nonlinear Spiking Motoneurons for Powering Up Locomotion

Rémi Bos,[1] Ronald M. Harris-Warrick,[2] Cécile Brocard,[1] Liliia E. Demianenko,[4] Marin Manuel,[3] Daniel Zytnicki,[3] Sergiy M. Korogod,[4] and Frédéric Brocard[1,5,*]
[1]Institut de Neurosciences de la Timone (UMR7289), Aix-Marseille Université and Centre National de la Recherche Scientifique (CNRS), Marseille, France
[2]Department of Neurobiology and Behavior, Cornell University, Ithaca, NY, USA
[3]Centre de Neurophysique, Physiologie et Pathologie, UMR 8119, CNRS/Université Paris Descartes, 45 rue des Saints-Pères, 75270 Paris Cedex 06, France
[4]Bogomoletz Institute of Physiology, National Academy of Sciences of Ukraine, Kiev, Ukraine
[5]Lead Contact
*Correspondence: frederic.brocard@univ-amu.fr
https://doi.org/10.1016/j.celrep.2018.02.093

SUMMARY

Spinal motoneurons are endowed with nonlinear spiking behaviors manifested by a spike acceleration whose functional significance remains uncertain. Here, we show in rodent lumbar motoneurons that these nonlinear spiking properties do not rely only on activation of dendritic nifedipine-sensitive L-type Ca^{2+} channels, as assumed for decades, but also on the slow inactivation of a nifedipine-sensitive K^+ current mediated by Kv1.2 channels that are highly expressed in axon initial segments. Specifically, the pharmacological and computational inhibition of Kv1.2 channels occluded the spike acceleration of rhythmically active motoneurons and the correlated slow buildup of rhythmic motor output recorded at the onset of locomotor-like activity. This study demonstrates that slow inactivation of Kv1.2 channels provides a potent gain control mechanism in mammalian spinal motoneurons and has a behavioral role in enhancing locomotor drive during the transition from immobility to steady-state locomotion.

INTRODUCTION

Spinal motoneurons are nonlinear integrators of the locomotor network (Brownstone, 2006; Heckman et al., 2008). The most distinctive nonlinear firing property consists of a self-sustained firing evoked by a brief excitation (Hounsgaard and Mintz, 1988; Hultborn et al., 2013). This all-or-none bistable behavior arises from a prolonged depolarization known as a "plateau potential," which is mediated by persistent inward currents (Bouhadfane et al., 2013; Hounsgaard et al., 1984; Kiehn and Harris-Warrick, 1992; Schwindt and Crill, 1980). From extensive *in vitro* recordings, the plateau potential appears to be preceded by a slow subthreshold membrane depolarization, then manifested by a spike-frequency acceleration before reaching a steady-state firing rate (Bennett et al., 2001; Conway et al., 1988; Hounsgaard and Kiehn, 1989; Leroy et al., 2014) referred to as the "preferred firing range" (Kiehn and Eken, 1997). Analogous firing-frequency acceleration, seen in motor units from *in vivo* recordings, provides evidence that the slow voltage transition to plateau is part of the physiological repertoire of motoneurons (Collins et al., 2002; Eken et al., 2008; Kiehn and Eken, 1997; Nickolls et al., 2004). The other striking manifestation of the slow voltage transition to the plateau potential is the cumulative depolarization of the membrane potential and slow increase in spiking frequency with repetitive excitations at short intervals (Bennett et al., 1998a, 1998b; Svirskis and Hounsgaard, 1997), as occurs during locomotion (Brownstone et al., 1994). This apparent short-term memory is usually referred to as a "windup" phenomenon. *In vivo* correlates are found in the form of a progressive amplification of both motor unit discharges and force development during the onset of repetitive movements like locomotion (Bennett et al., 1998a; Collins et al., 2002; Gorassini et al., 1999, 2002; Hornby et al., 2003; Kiehn and Eken, 1997; Nickolls et al., 2004).

The slow voltage transition to the plateau is assumed to rely on progressive recruitment of L-type Ca^{2+} channels, because both spike-frequency acceleration and windup are blocked by the L-type channel blocker nifedipine in motoneurons (Hornby et al., 2002; Hounsgaard and Kiehn, 1989; Hounsgaard and Mintz, 1988; Hsiao et al., 1998; Svirskis and Hounsgaard, 1997). However, the involvement of L-type Ca^{2+} channels has significant limitations during early developmental stages because both spike-frequency acceleration and windup emerge as early as birth in motoneurons of neonatal rats (Bouhadfane et al., 2013) when L-type Ca^{2+} channels are not or only weakly expressed (Gao and Ziskind-Conhaim, 1998; Jiang et al., 1999). This offset suggests that channels other than L-type Ca^{2+} channels may contribute to the appearance of nonlinear properties during early developmental stages. The present study demonstrates in rats and mice that the slow voltage transition to plateaus is mainly mediated by the slow inactivation of a nifedipine-sensitive K^+ current through Kv1.2 channels. Furthermore, we take a step toward identifying a behavioral role for Kv1.2 channels in the windup of rhythmic motor outputs upon the initiation of locomotion.

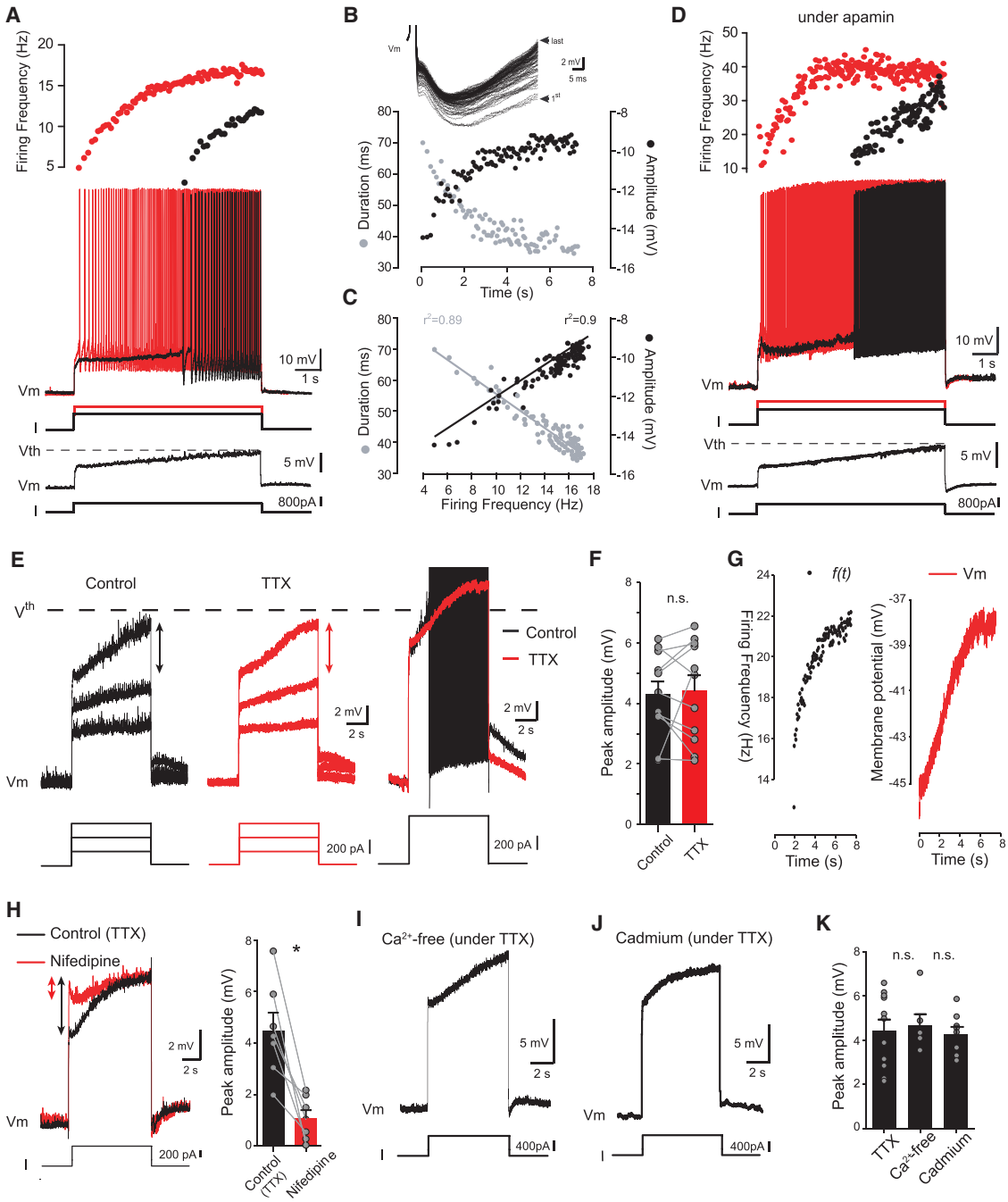

Figure 1. The Delayed Spike-Frequency Acceleration from Bistable Motoneurons Reflects Basic Features of a TTX-Insensitive Slow Membrane Depolarization

(A) Superimposition of representative voltage traces in response to subliminal (bottom), liminal (middle black), or supraliminal (middle red) depolarizing pulses. Instantaneous frequency plots on top of intracellular recordings.

(B) Time-course changes in duration (gray dots, left y axis) and amplitude (black dots, right y axis) of afterhyperpolarizations (AHPs) during tonic spiking of the motoneuron illustrated in (A). (Top) Superimposed AHPs.

(C) Duration (gray dots, left y axis) and amplitude (black dots, right y axis) of AHPs as function of the firing frequency. Continuous lines are the best-fit linear regression. ***$p < 0.001$, Spearman correlation test. r indicates the correlation index.

(D) Similar recordings as in (A) under apamin (100 nM).

(E) Superimposed voltage traces in response to subliminal (left and middle) or supraliminal (right) depolarizing pulses before (black) and during (red) TTX (1 μM). The dotted line illustrates the spiking threshold (V^{th}).

(F) Mean peak amplitude of slow membrane depolarizations (4.3 ± 0.4 mV for control versus 4.4 ± 0.5 mV during TTX, n = 11 cells). $p > 0.05$, Wilcoxon paired test.

(legend continued on next page)

RESULTS

Delayed Spike-Frequency Acceleration: A Hallmark of Bistability Both in Neonatal and Adult Motoneurons

Under *in vitro* recording conditions with temperature >30°C and 1.2 mM $CaCl_2$ in the saline as found *in vivo* (Fowler and Kellogg, 1975; Jones and Keep, 1988), up to 80% of neonatal motoneurons recorded in whole-cell mode from 4th/5th lumbar spinal cord slices display bistability, manifested by self-sustained spiking after a brief excitation (Bouhadfane et al., 2013). In response to subthreshold current steps, bistable lumbar motoneurons (n = 28 cells) invariably developed a voltage-dependent slow membrane depolarization triggered at −69.2 ± 0.6 mV. Close to the rheobase (888 ± 75 pA), the slow depolarization increased monoexponentially with a time constant of 4.6 ± 0.5 s (Figure 1A, bottom trace), and its maximum amplitude was 4.8 ± 0.3 mV. Slightly above rheobase, the ramp depolarization culminated in a delayed onset of spike discharge characterized by a net spike-frequency acceleration (Figure 1A, top black trace). Incremental depolarizing pulses reduced the delay until conversion to tonic spiking (Figure 1A, top red trace). The delayed firing occurred within a range of 1.00–1.25 ± 0.2 times the rheobase. At intermediate current pulses, some motoneurons (6 of 28) fired a burst of spikes at current onset, separated from tonic spiking by a pause (Figure S1A). During sustained discharge induced by a mean current of 1,100 ± 90 pA, spike frequency increased from 15.3 ± 0.8 to 24.8 ± 0.3 Hz until a steady-state rate was achieved without further apparent adaptation ($p < 0.001$; Figure S1B). During the discharge, motoneurons' action potentials exhibited a progressive decrease of both duration and amplitude of the slow afterhyperpolarization ($p < 0.001$; Figure 1B; Figures S1C and S1D). These decreases paralleled the time course of acceleration of the firing frequency (Figure 1C; Figures S1E and S1F). Importantly, non-bistable motoneurons did not display either a voltage-dependent slow membrane depolarization or delayed spike-frequency acceleration. To determine whether this delayed firing pattern was a transitory developmental phenomenon, we recorded the firing properties of lumbar motoneurons from adult mice *in vivo*. Similar to the neonatal *in vitro* recordings, the majority of motoneurons (22 out of 30) displayed a slow membrane depolarization (Figure S2A) and started to fire with a delay from pulse onset. Once firing had started, the instantaneous firing frequency increased over time (Figure S2B).

Delayed Spike-Frequency Acceleration Reflects a TTX-Insensitive Slow Membrane Depolarization

We investigated the cellular mechanisms underlying the spike-frequency acceleration in neonatal rat motoneurons. Although the tight relationship between the time course of the afterhyperpolarization and discharge acceleration supports a role for Ca^{2+}-activated K^+ channels, their blockade by apamin did not abolish either the delayed spike-frequency acceleration or the subthreshold slow membrane depolarization (Figure 1D; Figures S3A–S3C). The slow membrane depolarization is not dependent on a subthreshold-activated persistent Na^+ inward current because it was not affected by tetrodotoxin (TTX; 1 μM), a blocker of voltage-gated Na^+ channels ($p > 0.05$; Figures 1E and 1F). Notably, the firing rate increase recorded before the application of TTX could be superimposed on the TTX-resistant slow membrane depolarization (Figure 1G). We thus considered that the apparent spike-frequency acceleration reflects basic features of the slow membrane depolarization independent of voltage-gated Na^+ channels.

Subsequent experiments were conducted under TTX in order to determine the ionic basis of the slow membrane depolarization. Nifedipine (20 μM), a blocker widely used to demonstrate the contribution of L-type Ca^{2+} channels, significantly decreased the slow membrane depolarization ($p < 0.05$; Figure 1H). However, no sign of persistent inward Ca^{2+} current was clearly observed in our recordings (Figure S3D). Furthermore, the slow depolarization did not differ when recorded in Ca^{2+}-free solution or in the presence cadmium (100 μM), a broad-spectrum Ca^{2+} channel blocker ($p > 0.05$; Figures 1I–1K). Neither the blockade of T-type Ca^{2+} channels by mibefradil (10 μM) nor intracellular Ca^{2+} chelation (1,2-bis(o-aminophenoxy)ethane-N,N,N′,N′-tetraacetic acid [BAPTA], 10 mM) affected the slow depolarization ($p > 0.05$; Figures S3E and S3F). We thus assumed that nifedipine did not block the slow depolarization by inhibiting Ca^{2+} influx, but by some other mechanism. In sum, both Ca^{2+}-activated K^+ channels and voltage-gated Ca^{2+} channels do not appear as major contributors of the TTX-insensitive slow membrane depolarization.

The Slow Membrane Depolarization Is Mediated by Slow Inactivation of a TEA-Insensitive K^+ Current

In normal artificial cerebrospinal fluid (aCSF), during the spike-frequency acceleration, the action potential broadened monoexponentially ($p < 0.001$; Figures 2A and 2B; Figure S4A). At the same time, the rise slope of spikes decreased linearly ($p < 0.01$; Figure 2C; Figure S4B), while the rate of repolarization monoexponentially slowed ($p < 0.001$; Figure 2D; Figure S4C) and was linearly related to the time course of increase of both the duration of spikes (Figure 2E; Figure S4D) and the spike-frequency acceleration (Figure 2F; Figure S4E). This result led us to suspect that the spike-frequency acceleration and the slow membrane depolarization may be caused by a very slow inactivation of a K^+ current. Under TTX, the broad-spectrum

(G) TTX-resistant slow membrane depolarization (left, black dots) recorded in (E) and time-course changes in instantaneous frequency of spikes (right, red line) recorded before TTX.

(H) Superimposed voltage traces under TTX in response to a depolarizing pulse before (black) and during (red) nifedipine (20 μM). (Right) Mean of slow membrane depolarizations (4.5 ± 0.7 mV for control versus 1.1 ± 0.3 mV during nifedipine, n = 7 cells). *$p < 0.05$, Wilcoxon paired test.

(I and J) Representative slow membrane depolarizations under TTX recorded either in Ca^{2+}-free solution (I) or in the presence of cadmium (100 μM) (J).

(K) Mean peak amplitude of slow membrane depolarizations (TTX: 4.4 ± 0.5 mV, n = 14 cells; Ca^{2+}-free: 4.7 ± 0.5 mV, n = 6 cells; cadmium: 4.3 ± 0.3 mV, n = 8 cells). $p > 0.05$, one-way ANOVA.

Data are mean ± SEM. See also Figures S1–S3.

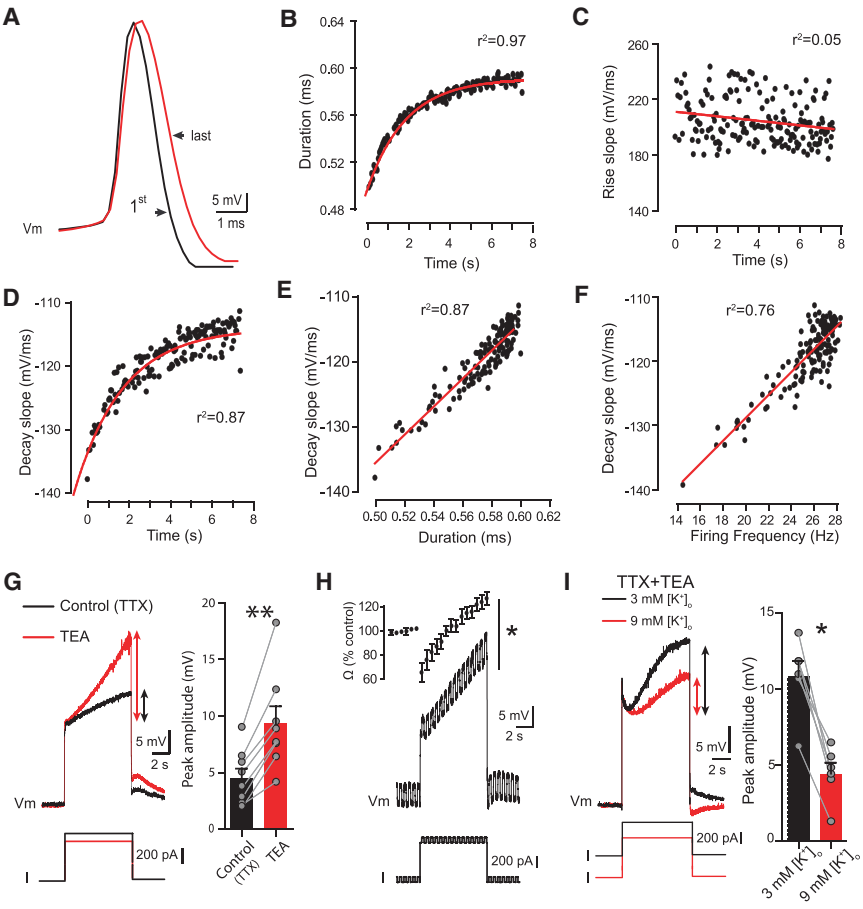

Figure 2. Slow Membrane Depolarization in Neonatal Rat Motoneurons Is Dependent on TEA-Insensitive Voltage-Gated K^+ Channels

(A) Superimposition of the first (black trace) and the last spike (red trace) from tonic spiking of the motoneuron illustrated in Figure 1A.

(B–D) Time-course changes in half-width duration (B), rise slope (C), and decay time (D) during tonic spiking.

(E and F) Decay slope as function of the duration (E) or the firing frequency (F) of spikes. Continuous red lines in (B)–(F) are the best-fit linear or nonlinear regression. r indicates the correlation index.

(G) Superimposed voltage traces in response to a depolarizing pulse before (black trace) and during (red trace) TEA (10 mM). (Right) Mean peak amplitude of slow membrane depolarizations (4.5 ± 0.8 mV for control versus 9.4 ± 1.5 mV during TEA, n = 8 cells). **p < 0.01, Wilcoxon paired test.

(H) Representative voltage trace in response to a long-lasting depolarizing pulse superimposed by brief depolarizing pulses. (Top) Relative time course changes in the membrane resistance of motoneurons (n = 7 cells). *p < 0.05, comparing input resistance at the onset (100% ± 18%) and at the end (187% ± 18%) of the long-lasting pulse, n = 7 cells, Wilcoxon paired test.

(I) Superimposed voltage traces before (black trace) and after (red trace) raising $[K^+]_o$ from 3 to 9 mM. (Right) Mean peak amplitude of slow membrane depolarizations (10.8 ± 1.0 mV in 3 mM $[K^+]_o$ versus 4.4 ± 0.7 mV in 9 mM $[K^+]_o$, n = 7 cells). *p < 0.05, Wilcoxon paired test.

Data are mean ± SEM. See also Figure S4.

voltage-gated K^+ channel blocker tetraethylammonium (TEA) increased the amplitude of the slow membrane depolarization ($p < 0.01$; Figure 2G). Thus, TEA-sensitive K^+ currents appear to counteract the slow membrane depolarization. However, after an initial decrease by 34% ± 8% caused by the depolarizing step, the cell input resistance slowly increased by 87% ± 18% in parallel with the emergence of the slow depolarization ($p < 0.05$; Figure 2H). A slow decrease in membrane conductance accompanying a slow depolarization may be consistent with the slow inactivation of TEA-insensitive K^+ channels. This hypothesis is further supported by a decrease in amplitude of the slow membrane depolarization when the extracellular K^+ concentration was raised to 9 mM, which reduced the driving force on potassium in this voltage range ($p < 0.05$; Figure 2I).

To further decipher the ionic mechanisms underlying the slow depolarization, we switched to voltage-clamp mode in the presence of TTX and TEA. When subjected to a depolarizing voltage step from −80 to −40 mV for 7.5 s, motoneurons displayed a prominent outward current, slowly inactivating with a decay time constant of 4.1 ± 0.2 s similar to that found for the slow membrane depolarization (Figure 3A). The outward current was decreased in amplitude when $[K^+]_o$ was increased to 9 mM ($p < 0.05$; Figure 3A) and was abolished when the intrapipette K^+ was replaced by cesium ($p < 0.05$; Figure 3B), suggesting that the measured current was primarily carried by K^+ ions. Consistent with this, the reversal potential for the current was close to the predicted equilibrium potential for K^+ (−87.7 ± 4.3 mV; Figure S5A). We refer to this current as slow inactivating potassium outward current (I_{Ks}). Note that I_{Ks} remained stable when whole-cell recordings were established (Figure S5B).

Biophysical Properties of I_{Ks} Responsible for the Slow Membrane Depolarization

Experiments were undertaken on seven motoneurons to examine the voltage dependence of the channel(s) underlying I_{Ks}. From the current-voltage relationship fitted with a standard Boltzmann function (Figure 3C, black traces), its threshold for activation was positive to −70 mV, and its amplitude increased steeply (slope factor k: 7.5 ± 0.7) for larger voltage steps with a mid-point of activation ($V_{1/2}$) at −43 ± 2 mV and then plateaued above −20 mV (Figure 3D). The voltage dependence of inactivation was studied with a series of depolarizing presteps followed by measurement of the remaining current at −40 mV (Figure 3C, gray traces); I_{Ks} was half-inactivated at −51.9 ± 2.2 mV and fully inactivated when the membrane potential was maintained above −30 mV (Figure 3D). Recovery from inactivation was very slow: complete recovery of the initial amplitude potassium current required separation of two successive long-lasting current pulses by at least 12 s (Figures 3E and 3F). In line with the slow recovery from inactivation, the delay between the onset

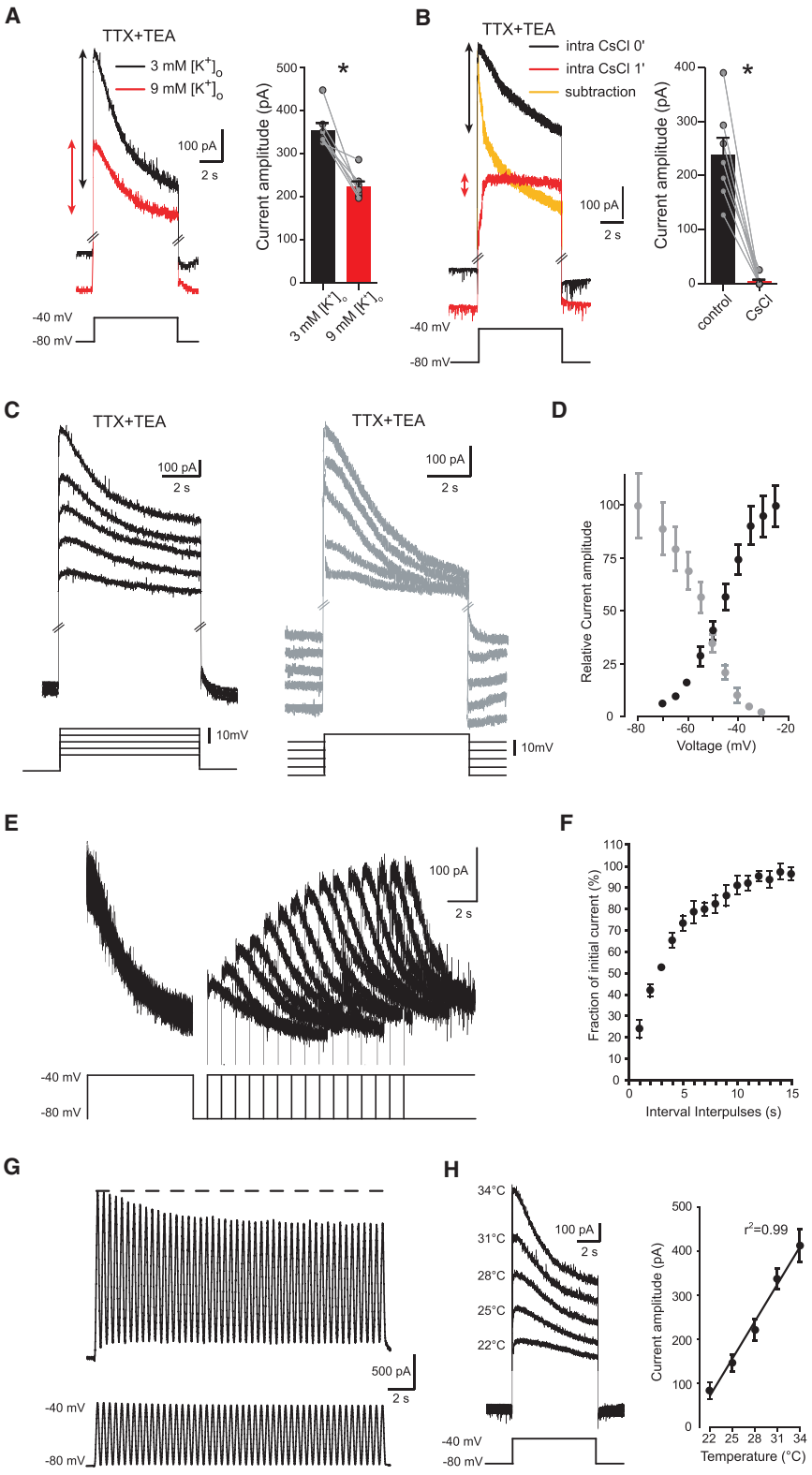

Figure 3. Biophysical Properties of Voltage-Gated K^+ Channel(s) Responsible for the Slow Membrane Depolarization

(A and B) Superimposed outward currents elicited by a depolarizing step before and after extracellular perfusion of a medium containing 9 mM $[K^+]_o$ (A) or after intracellular dialysis of cesium chloride (1 mM, (B). (Right panels) Mean of current amplitude of slow inactivating outward currents indicated by the vertical arrows (354.1 ± 16.3 pA in 3 mM $[K^+]_o$ versus 223.6 ± 11.5 pA in 9 mM $[K^+]_o$, n = 7 cells; 236 ± 13.8 pA for control versus 0.40 ± 0.08 pA for CsCl, n = 7 cells). *p < 0.05, Wilcoxon paired test.

(C) Superimposed outward currents elicited by voltage steps from holding potential of −80 mV (left) or by stepping to the membrane potential of −20 mV from a series of holding potentials (right).

(D) Activation (black dots) and steady-state inactivation (gray dots) curves of outward currents (n = 7 cells).

(E) Recovery of outward currents from inactivation. The initial depolarization was followed by a second similar depolarizing step of same amplitude having interpulse interval from 1 to 15 s.

(F) Mean values of the fractional recovery as function of interpulse intervals normalized to the amplitude of the outward current elicited by the first depolarizing step.

(G) Representative outward current in response to voltage oscillations (0.5 Hz). In means, outward currents declined by 269.3 ± 30.2 pA, n = 6 cells. *p < 0.05, Wilcoxon paired test.

(H) Left panel: superimposed outward currents in response to a depolarizing pulse as a function of bath temperature (n = 5 cells). Right panels: mean current amplitude of slow inactivating outward currents as a function of temperature. Continuous line is the best-fit linear regression. r indicates the correlation index. All recordings are performed in the presence of TTX (1 μM) and TEA (10 mM).

Data are mean ± SEM. See also Figure S5.

of the pulse and the onset of firing shortened in motoneurons from adult mice *in vivo* when the interval between two successive pulses was below 10 s, reflecting the reduction in I_{Ks} during the second step at these shorter intervals (Figures S2B and S2C). A cumulative inactivation was also found with repeated short depolarizations. Thus, I_{Ks} declined by 24% ± 5.7% when motoneurons were submitted to sinusoidal current injections at a frequency as low as 0.5–1 Hz ($p < 0.05$; Figure 3G). Note that the magnitude of I_{Ks} linearly increased with temperature (Figure 3H) and was similar in identified motoneurons innervating the triceps surae or the tibialis anterior muscles (Figure S5C). In sum, irrespective of their functional identity, most motoneurons displayed a slow-inactivating temperature-sensitive K^+ current likely responsible for the slow membrane depolarization.

The Pharmacological Profile of I_{Ks} Implicates Kv1.2 Channels

To provide insight into the α subunits forming the K^+ channel(s), we applied a battery of K^+ channel blockers in the presence of TTX and TEA. As a first observation, increasing the concentration of TEA from 10 to 20 mM did not further change I_{Ks}, suggesting that 10 mM was enough to block almost all TEA-sensitive K^+ channels ($p > 0.05$; Figure S5D). In addition to blocking L-type Ca^{2+} channels, nifedipine inhibits a variety of K^+ channels, including Kv1.1, Kv1.2, Kv1.3, Kv1.5, Kv2.1, and Kv3.1 (Grissmer et al., 1994; Li et al., 2015). Nifedipine (20 μM) caused a reduction of I_{Ks} ($p < 0.05$; Figure 4A; Table S1) and an inward shift of the holding current by −145 ± 30 pA ($p < 0.05$, n = 7 cells; Figure 4A). Spinal motoneurons of rats express Kv2.1 channels (Muennich and Fyffe, 2004), but their inhibition by stromatoxin (Escoubas et al., 2002) (STx; 3 μM) did not affect I_{Ks} ($p > 0.05$; Figure 4B; Table S1).

After the pharmacological exclusion of Kv2 subunits, we assessed the response to 4-AP for which Kv1 channels are sensitive (Coetzee et al., 1999). 4-Aminopyridine (4-AP; 0.2 mM) reduced I_{Ks} by the same amount as nifedipine ($p < 0.05$; Figure 4C; Table S1). To further investigate which Kv1 subunits are involved, we tested dendrotoxin-I (DTx-I; 1 μM), which blocks Kv1 channels that contain at least one Kv1.1 or Kv1.2 subunit (Grissmer et al., 1994). DTx-I reversibly abolished I_{Ks} ($p < 0.01$; Figure 4D; Table S1). Immunostaining substantiates the presence of Kv1.1 (Figures 4E and 4G) and Kv1.2 (Figures 4H–4J) channels in almost all presumptive neonatal motoneurons (57 out of 62 cells for Kv1.1; 62 out of 66 for Kv1.2), specifically in the distal part of their Ankyrin G-positive axonal initial segments. Both subunits were abundantly co-expressed in the vast majority of presumptive motoneurons (45 out of 49 cells; Figures 4K–4M).

To provide further clues about the channel subunit composition, we used toxins specific for one Kv1 subunit. Application of dendrotoxin-K (DTx-K; 1 μM), a potent blocker for Kv1.1 (Robertson et al., 1996), had no effect ($p > 0.05$; Figure 4N; Table S1), while tityustoxin (TsTX; 1 μM), which inhibits Kv1.2 (Werkman et al., 1993), reversibly suppressed I_{Ks} ($p < 0.01$; Figure 4O; Table S1) and the slow depolarization it underlies (Figures 5A and 5B). Taken together, these data strongly implicate inactivation of potassium channels containing Kv1.2 subunits in the generation of I_{Ks}.

Inactivation of Kv1.2-Mediated I_{Ks} Promotes Near-Threshold Nonlinear Firing Properties in Motoneurons

We tested the functional role of Kv1.2 channels on firing properties of bistable motoneurons by measuring their degree of spike-frequency acceleration before and after bath application of TsTX. Experiments were performed in the presence of the glutamate receptor blocker kynurenate (1.5 mM) to dampen neural network activity when Kv1.2 channels were blocked. As a first observation, bath application of TsTX increased the holding current required to maintain the membrane potential at –80 mV ($p < 0.05$; Table S2), consistent with the block of a Kv1.2-mediated conductance that is active at rest. As mentioned above, TsTX prevented or strongly decreased the slow membrane depolarization associated with I_{Ks} (Figures 5A and 5B), as well as the delay in onset of firing, which can be observed across a narrow range of low-voltage steps up to 1.08 ± 0.06 times the rheobase (Figure 5C). In addition, the motoneuron's slow acceleration of firing during tonic spiking was abolished with TsTX (Figures 5D and 5E); the neurons' initial spike frequency was in the range of the maximal frequency seen at the end of the firing acceleration in untreated neurons. We further tested the role of Kv1.2 channels in the integration of rhythmic inputs, by investigating the motoneurons' responsiveness to sine wave current injection of constant amplitude with temporal dynamics compatible with locomotor frequencies (0.5–2 Hz). In the subthreshold range, close to the rheobase, the voltage response of untreated motoneurons to eight successive same-amplitude cycles increased by 4.6 ± 0.4 mV ($p < 0.01$; Figure 5F), which was similar to the peak amplitude of the slow membrane depolarization seen in response to a rectangular current injection. When current was increased to reach the firing threshold, the first spike seen was elicited in response to the third or fourth cycle in the series (Figure 5G), and increased in frequency with each subsequent cycle. During application of TsTX, the slow accumulating depolarization of subthreshold oscillatory membrane potentials was occluded by TsTX ($p < 0.01$; Figure 5F); the response to the first cycle was the same as for all other cycles. Likewise, the delay of firing in response to successive oscillatory cycles disappeared (Figure 5G); the neurons fired at maximal frequency during the first oscillation. Note that all results described above are reproduced by 1 μM DTx-I (Figure S6; Table S2).

Kv1.2-Mediated I_{Ks} Boosts Fictive Locomotion

To investigate the theoretical effect of Kv1.2 channels on motoneuron firing behavior, we used a multi-compartment computational model of the motoneuron. In this model, transient and persistent Na^+ currents, voltage-dependent delayed rectification and Ca^{2+}-dependent K^+ currents, and N-type Ca^{2+} current were simulated. Because the L-type Ca^{2+} current is not or only weakly expressed during the perinatal period (Gao and Ziskind-Conhaim, 1998), it was not included in the model. The model was further supplemented by a slowly inactivating Kv1.2-like conductance derived from our voltage-clamp recordings (Figures 3 and S7A–S7C). Simulated motoneurons expressing such currents reproduced key features of the biological responses to stepwise and sinusoidal depolarizing currents, i.e., a delayed firing pattern to small current steps (Figure 6A) and windup (increasing depolarization and acceleration of spiking)

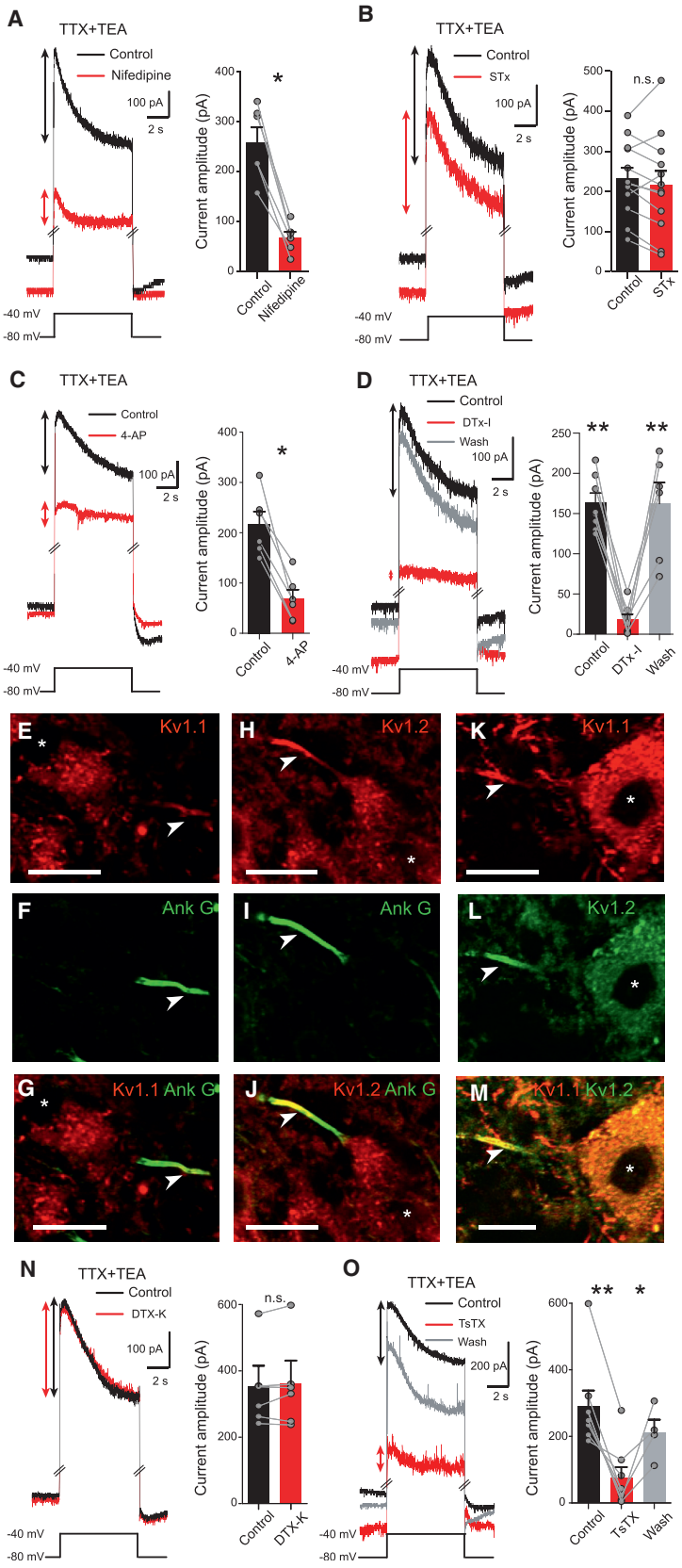

Figure 4. The Pharmacological Profile of the Outward Current Associated with Immunostaining Implicates Kv1.2 Channels

(A–D) Superimposed outward currents in response to a depolarizing pulse before (black trace) and during (red trace) nifedipine (20 μM) (A), stromatoxin (STx; 3 μM) (B), 4-aminopyridine (4-AP; 0.2 mM) (C), or dendrotoxin-I (DTx-I; 1 μM) (D). On right of all panels, mean amplitude of slow inactivating outward currents indicated by the vertical arrows (259 ± 25 pA for control versus 60 ± 12 pA during nifedipine, n = 6 cells; 232 ± 27 pA for control versus 216 ± 35 pA during STx, n = 12 cells; 217 ± 25 pA for control versus 68.6 ± 18.2 pA during 4-AP, n = 6 cells; 163.7 ± 11.7 pA for control versus 18.4 ± 6.4 pA during DTx-I versus 162.5 ± 26.1 pA in washout, n = 8 cells). $p > 0.05$; *$p < 0.05$; **$p < 0.01$, Wilcoxon paired test in (A)–(C), one-way ANOVA with repeated measures in (D).

(E–J) Immunostaining of Kv1.1 (E) (n = 66 cells) or Kv1.2 (H, n = 62 cells) along the axon initial segments of neonatal rat lumbar motoneurons (L4-L5) labeled by the ankyrin G antibody (F and I). Kv1.1 and ankyrin G are merged in (G), and Kv1.2 and ankyrin G are merged in (J).

(K–M) Double immunostaining of Kv1.1 (K) and Kv1.2 (L) along the axon initial segments of neonatal rat lumbar motoneurons (L4-L5, n = 49 cells). Both are merged in (M). Asterisks indicate the nucleus of motoneurons. Arrowheads show axon initial segments. Scale bars, 20 μm.

(N and O) Superimposed outward currents in response to a depolarizing pulse before (black trace) and during (red trace) dendrotoxin-K (DTx-K; 1 μM) (N) or during tityustoxin (TsTX; 1 μM) (O). (Right panels) Mean amplitude of slow inactivating outward currents indicated by the vertical arrows (350.9 ± 53.6 pA for control versus 358.6 ± 57.8 pA during DTx-K, n = 6 cells; 291.5 ± 46.2 pA for control versus 75.6 ± 32.3 pA during TsTX versus 210.7 ± 39.7 pA during washout, n = 8 cells). $p > 0.05$; *$p < 0.05$; **$p < 0.01$, Wilcoxon paired test in (N), one-way ANOVA with repeated measures in (O). All recordings are performed in the presence of TTX (1 μM) and TEA (10 mM). Data are mean ± SEM.

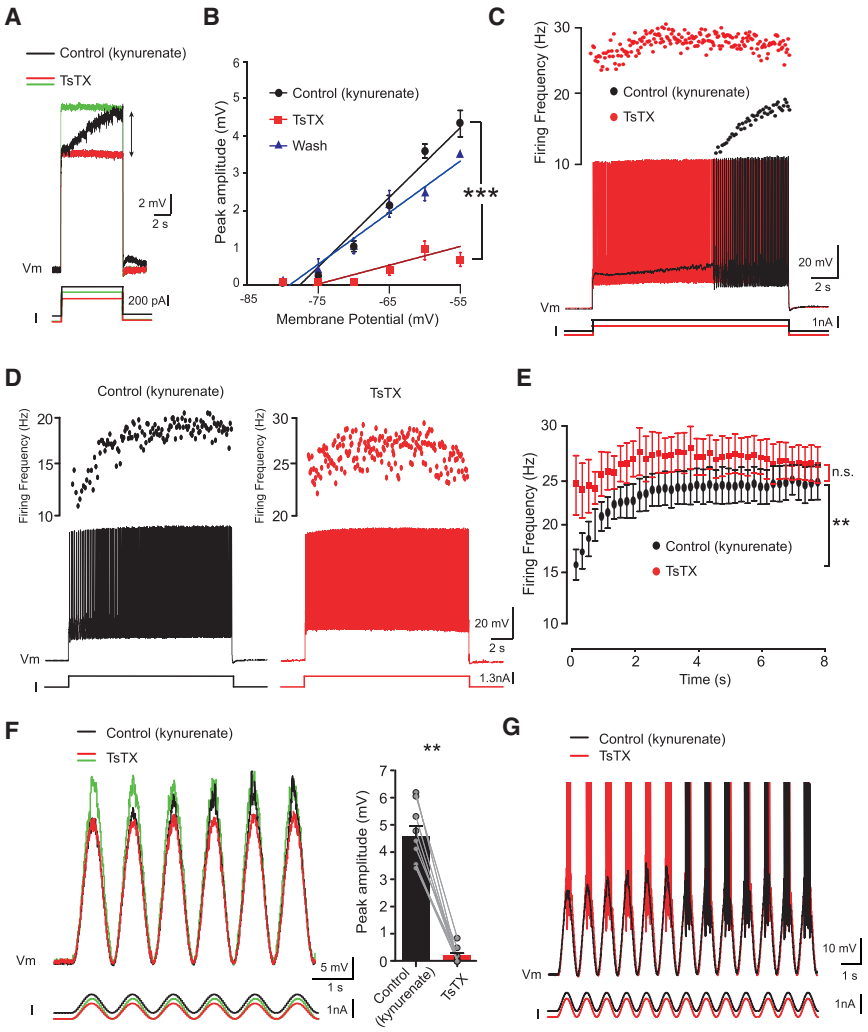

Figure 5. Slow Inactivation of Kv1.2 Channels Promotes Near-Threshold Nonlinear Firing Properties in Bistable Motoneurons

(A) Superimposed voltage traces in response to subliminal depolarizing pulse before (black trace) and during (red and green traces) tityustoxin (TsTX; 1 μM).

(B) Mean amplitude of slow depolarizations from seven motoneurons as function of the membrane potentials before TsTX (black), during TsTX (red), and after washout (blue). Mean peak amplitude (4.4 ± 0.5 mV for control; 0.83 ± 0.17 mV during TsTX; 3.6 ± 0.08 mV after washout). ***$p > 0.001$, one-way ANOVA with repeated measures. Continuous lines are the best-fit linear regression.

(C and D) Representative voltage traces in response to a liminal (C) or supraliminal (D) depolarizing pulse before (black trace) and during TsTX (red trace). Instantaneous frequency plots on top of intracellular recordings.

(E) Mean time-course changes in instantaneous firing frequency from all recorded motoneurons before (black) or during TsTX (red) in response to a supraliminal depolarizing pulse (n = 7 cells). Instantaneous firing frequency changes from 16 ± 1.5 to 25.1 ± 1.7 Hz before TsTX and from 24 ± 3 to 26 ± 1.8 Hz during TsTX. $p > 0.05$; **$p < 0.01$, Wilcoxon paired test.

(F and G) Representative voltage traces before (black trace) and during TsTX (red and green traces) in response to subliminal (F) or liminal (G) oscillatory currents (1 Hz). (F, right panel) Mean peak amplitude increases of membrane oscillations (4.6 ± 0.4 mV for control versus 0.2 ± 0.1 mV, n = 9 cells). **$p < 0.01$, Wilcoxon paired test. Spikes in (G) are truncated. All recordings are performed under kynurenate (1.5 mM). Note that under TsTX a bias current was used to maintain the pre-pulse membrane potential at the holding potential fixed in control condition. For a direct comparison, current pulses were also adjusted to reach the same level of depolarization at the onset of the pulse as that for control (red trace in F). Note a same current amplitude as in control was also injected (green trace in F).

Data are mean ± SEM. See also Figure S6.

during repeated oscillations (Figure 6B). Both phenomena were abolished if Kv1.2 current was "off," mimicking the effects of TsTx (Figures 6C and 6D). Note that the delay between current onset and firing onset was shortened when time constant of the Kv1.2 current inactivation was accelerated (Figures S7D–S7G). In sum, the model supplemented with Kv1.2 current captures key features of near-threshold nonlinear spiking properties of motoneurons, making it suitable to use as a tool to explore how Kv1.2 channels might shape motor outputs during rhythmic activity such as locomotion.

We simulated a population of 50 uncoupled motoneurons that received sinusoidal stimuli representing incoming locomotor drive from the central pattern generator. To provide a necessary heterogeneity in firing properties of motoneurons, the half-activation ($V_{1/2}$) of the Kv1.2 current was Gaussian-distributed using our experimental estimates of 42.6 ± 1.6 mV. In the population, both the sequential number of the effective cycle and the number of spikes generated in each cycle randomly varied due to intrapopulation variability of Kv1.2 properties (Figure 6E, lower panel). As a result, the integrated activity builds up cycle by cycle before reaching a steady-state level (Figure 6E, upper panel).

To confirm the predictive functional role of slow inactivation of Kv1.2 channels in progressively boosting locomotor outputs, we performed *ex vivo* experiments from whole-mount spinal cord preparations with fictive locomotion evoked by stimulation of sensory afferents from the cauda equina (Figure 7A). As previously observed (Brocard et al., 2013), when locomotor-like activity developed in response to repeated caudal stimuli, the rhythmic motor outputs recorded in L5 ventral roots showed typical windup, characterized by progressive increases in ventral root burst amplitude ($p < 0.01$; Figure 7B). Direct application of aCSF from a pipette located above the L5 ventral horn column on one side of the spinal cord did not disturb this windup of fictive locomotor outputs ($p < 0.05$; Figure 7C). By contrast, a similar

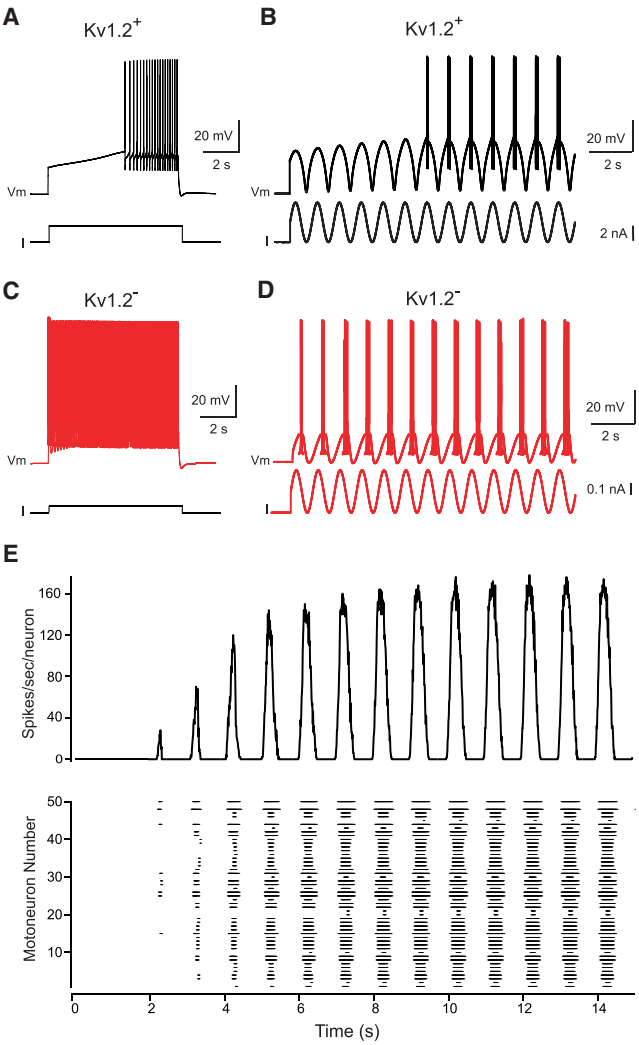

Figure 6. Firing Responses of Simulated Motoneurons to Steady and Oscillatory Depolarizing Inputs Suggest Essential Role of the Slow Inactivation of Kv1.2 Channels in Powering Up Locomotor Outputs

(A–D) Sequences of action potentials evoked by depolarizing current steps (A and C) or by 1-Hz sinusoidal depolarizing currents (B and D) applied at the soma in the conditions of Kv1.2 current switched "on" (A and B) and "off" (C and D). In (A), the slow inactivation time constant was adjusted to obtain a duration of the pre-firing depolarization similar to that recorded experimentally. (E) Activity of a population of 50 uncoupled simulated motoneurons receiving the same sinusoidal stimulation as in (B). Lower panel: raster plots of the spiking activity of individual cells where each horizontal line represents a neuron and each dot represents a spike. Upper panel: integrated population activity represented by the histogram of average number of spikes per second per neuron (bin width 10 ms). The motoneurons differed in the Kv1.2 current half-activation potential, which had a Gaussian distribution with mean ± SEM of 42.6 ± 1.6 mV corresponding to the experimental estimates.
See also Figure S7.

application of either nifedipine (20 μM) or tityustoxin (1 μM) significantly occluded the windup of L5 ventral root discharges ipsilateral to the application ($p > 0.05$; Figures 7D and 7E, red traces) without affecting the untreated contralateral side ($p < 0.01$; Figures 7D and 7E, black traces); the first burst of fictive locomotor output was near the maximal amplitude seen after windup in the unaffected side. Altogether, these results establish a functional role for inactivation of Kv1.2 channels in progressively amplifying the initial output of fictive locomotion.

DISCUSSION

The present study shows that dynamic changes in motoneuronal excitability can be attributed to slow inactivation of Kv1.2 channels under physiological conditions. We found that most lumbar motoneurons display a delayed spike-frequency acceleration, as previously observed in neonatal mice (Leroy et al., 2014; Pambo-Pambo et al., 2009) likely in the largest fast-type motoneurons (Durand et al., 2015; Leroy et al., 2014). Far from being exclusive to spinal motoneurons, this firing pattern has been described in brainstem motoneurons of neonatal rats (Russier et al., 2003) and adult guinea pigs (Nishimura et al., 1989). Here, we show that this delayed spiking in motoneurons is not transiently expressed, but persists in a similar proportion into adulthood, suggesting that it develops early and is maintained through life.

Regardless of species-specific features, many factors may account for their late discovery in adults. First, our stimulation protocol (long-lasting subthreshold current) that most clearly demonstrated the slow membrane depolarization is infrequently used *in vivo*. Second, most intracellular recordings from *in vitro* adult preparations are performed at room temperature, which limits the activation of Kv1.2 channels (Russell et al., 1994). Third, adult slice preparations may bias recordings to small motoneurons with high input resistances (Carp et al., 2008) because larger delayed firing motoneurons that have large dendritic trees (Leroy et al., 2014) may suffer more damage to dendrites during the slice procedure. Finally, other currents whose effects on the firing pattern are opposed to those of Iks, such as currents involved in the spike-frequency adaptation (Iglesias et al., 2011; Miles et al., 2005), could be differentially neuromodulated depending on the preparation and on the animal state.

The delayed spike-frequency acceleration in motoneurons is linked to a slow ramp depolarization. Some studies indicate that the spike-frequency acceleration results from imbalance between changing inward and outward currents (Nisenbaum et al., 1994; Nishimura et al., 1989). The present study suggests that, in neonatal motoneurons, the activation of persistent inward currents may be less important than the inactivation of a K^+ current. Perinatal motoneurons broadly express three types of K^+ current, including the Ca^{2+}-dependent K^+ current, the A-current, and a TEA-sensitive slow-inactivating K^+ current (Gao and Ziskind-Conhaim, 1998; Takahashi, 1990). While the last one may contribute to the slow depolarization in motoneurons (Leroy et al., 2015), we have identified a fourth K^+ current whose inactivation plays the major role in generating the slow depolarization, and thereby the nonlinear spiking acceleration. This K^+ current, here referred to as I_{Ks}, resembles in some ways the I_D current originally described in hippocampal cells (Storm, 1988): it is sensitive to 4-AP but insensitive to TEA, activates at subthreshold potentials, inactivates very slowly, and recovers from inactivation with a long time constant.

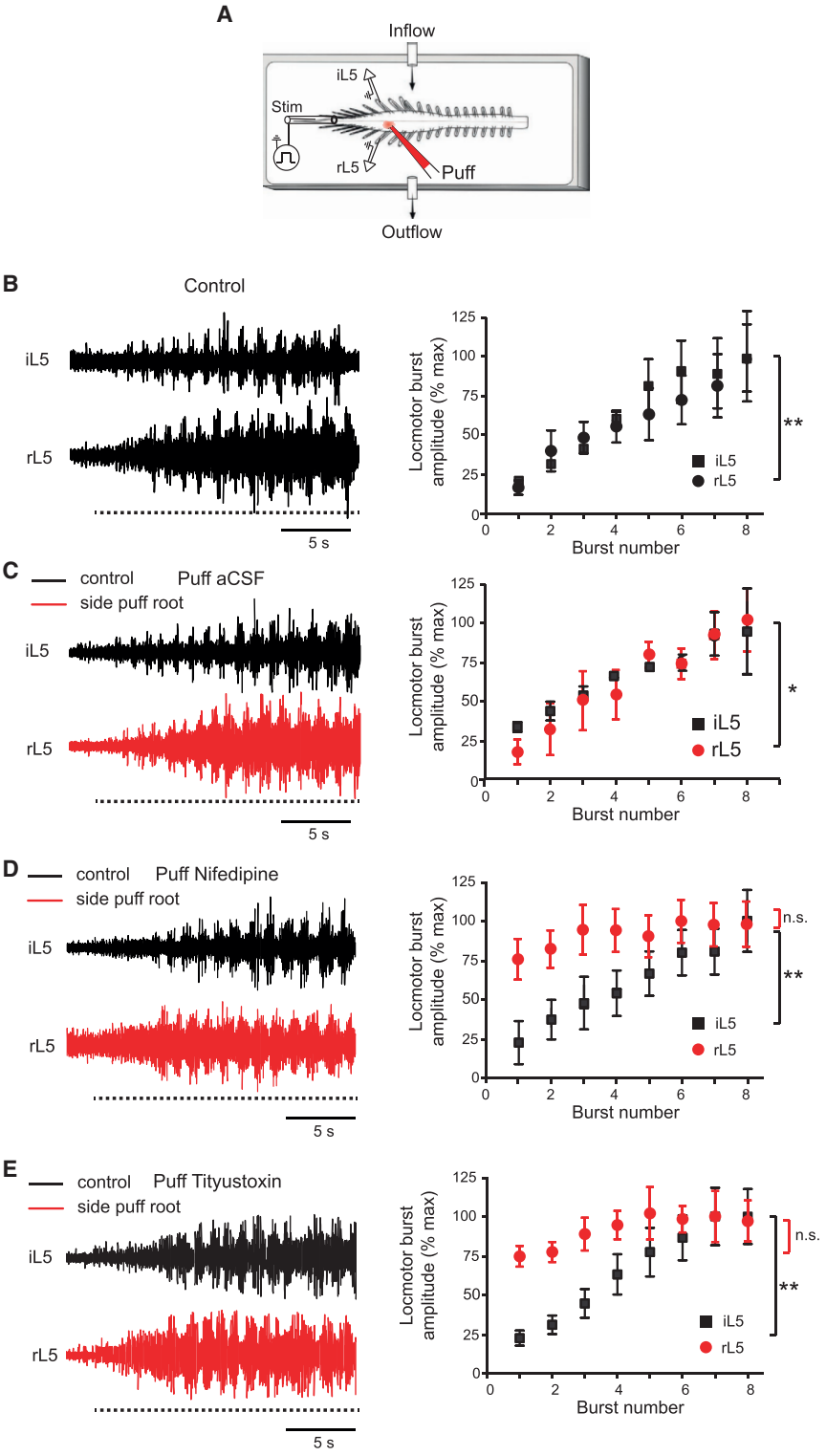

Figure 7. Slow Inactivation of Kv1.2 Potassium Channels for Powering Up Fictive Locomotor Outputs

(A) Drawing of the *in vitro* isolated spinal cord from neonatal rat illustrating lumbar (L5) ventral roots where the locomotor-like activity was recorded, and the localized ipsilateral application of drugs at the level of the L5 ventral horn. The caudal equina was stimulated (200–850 μA, 10–20 s, 1–4 Hz) to induce fictive locomotion.

(B–E) Raw traces of locomotor output recorded from right (rL5) and left (lL5) L5 ventral roots before (B) or after a brief local application of aCSF (C), nifedipine (D), or tityustoxin (E) above the ventral horn ipsilateral to rL5. Dashed lines represent the caudal equina stimulation. (Right panels) Time-course changes in amplitude of motor outputs during the initial phase of fictive locomotion. n = 4, 8, and 6 isolated spinal cords with aCSF, nifedipine, and tityustoxin, respectively. $p > 0.05$; $^{*}p < 0.05$; $^{**}p < 0.01$, Wilcoxon paired test. Data are mean ± SEM.

Our data point to Kv1.2 channel subunits as major contributors to I_{Ks} in neonates. First, I_{Ks} was eliminated by a Kv1.2-specific channel blocker and shows other pharmacological similarities with channels that contain Kv1.2 subunits. Second, immunostaining revealed that Kv1.2 channels were expressed in the initial segment of motoneurons. Third, a computational model endowed with a Kv1.2-like conductance reproduced motoneurons' nonlinear firing properties. Last, I_{Ks} has substantial similarities with the biophysical profile of the Kv1.2-encoded current in heterologous expression systems (Grissmer et al., 1994; Werkman et al., 1993).

Given the reported dependence of the firing frequency acceleration on L-type Ca^{2+} channels in adults (Hornby et al., 2002; Hounsgaard and Kiehn, 1989; Hounsgaard and Mintz, 1988; Hsiao et al., 1998; Svirskis and Hounsgaard, 1997), it is possible that I_{Ks} is a transient characteristic at a time when L-type Ca^{2+} channels are weakly expressed in neonatal rat motoneurons (Gao and Ziskind-Conhaim, 1998). Our data provide support to the view that adult motoneurons do express functional Kv1.2 channels. Although the pharmacological approach to assess their contribution is quite challenging *in vivo*, the delayed firing pattern mediated in neonates by Kv1.2 channels appears to be qualitatively similar to that recorded in adult motoneurons. Notably, the progressive reduction of the delayed onset of firing in response to repetitive stimuli fits well with the rate of slow recovery from inactivation of Kv1.2 channels. Consistent with our findings, adult lumbar motoneurons in mammals express both Kv1.2 channels in their initial segments (Duflocq et al., 2011; Rasband and Trimmer, 2001) and an unidentified

TEA-insensitive slow inactivating K^+ current (Schwindt and Crill, 1981). In sum, in adult motoneurons, Kv1.2 and L-type Ca^{2+} channels may have a complementary role in nonlinear firing properties; the L-type Ca^{2+} channels highly expressed in dendrites (Jiang et al., 1999) may amplify synaptic inputs, while inactivation of Kv1.2 channels highly expressed in initial segments (Duflocq et al., 2011; Rasband and Trimmer, 2001) may boost motoneuronal output.

I_{Ks} mediated by Kv1.2 channels powerfully regulates the excitability of motoneurons in many ways. We found it to contribute to setting the resting membrane potential, to shunt early excitation manifested by an initial pause in firing, or a pause before initiation of firing, and then to promote a slow acceleration in firing rate because of its slow inactivation. This spike frequency acceleration preceding the initiation of plateau potentials is a marker of bistable motoneurons attributed to activation of a nifedipine-sensitive L-type Ca^{2+}-current as well as persistent sodium and TRP-family calcium-activated nonselective (I_{CAN}) currents (Bouhadfane et al., 2013; Hornby et al., 2002; Hounsgaard and Kiehn, 1989; Hounsgaard and Mintz, 1988). It is not widely known that nifedipine also blocks potassium channels including Kv1.2 channels (Grissmer et al., 1994). In light of this and our results, Kv1.2 channels appear to be a significant determinant in the voltage transition to the plateau potential. We can reasonably assume that the slow inactivation of Kv1.2 channels provides the initial depolarization that in turn initiates the recruitment of persistent inward currents sustaining plateau potentials. Under this assumption, the slow inactivation of Kv1.2 channels may be the primary mechanism by which the plateau threshold is lowered during tonic synaptic excitation (Bennett et al., 1998b). Finally, another important feature of Kv1.2 channels is their slow recovery from inactivation, which provides to motoneurons a memory trace of their own activity. As a result, successive excitations in motoneurons become more efficient to reach the firing level (Leroy et al., 2015).

Genetic studies have supported the importance of Kv1.2 channels for motor function by linking their mutations to movement and gait disorders (Syrbe et al., 2015; Xie et al., 2010), but the cellular mechanism behind this was unclear. The present study provides insights into the operation of the locomotor network with a critical implication of Kv1.2 channels in adjusting the gain of motoneurons to behavioral needs. In motor tasks that involve repetitive movements such as locomotion, we show that the cumulative inactivation of Kv1.2 channels underlies windup of rhythmic motor outputs upon the initiation of fictive locomotion, as reported during the onset of step movements in cats (Jell et al., 1985) and humans (Gerasimenko et al., 2015). Kv1.2 channels may also contribute to the short-term potentiation of locomotor drives in motoneurons (Brownstone et al., 1994), somewhat reflected in the temporal facilitation of muscle activity produced by rhythmic muscle stretches in awake animals (Bennett et al., 1998a; Gorassini et al., 1999; Hornby et al., 2003) or by repetitive voluntary contractions or muscle vibrations in humans (Gorassini et al., 1998, 2002; Hornby et al., 2003; Romaiguère et al., 1993; Suzuki et al., 1990). In motor tasks that instead involve a tonic recruitment of motoneurons, such as during posture, we show that the slow inactivation of Kv1.2 initiates a voltage transition to a delayed nonlinear spiking activity and facilitates prolonged higher-frequency firing rates. Likewise, motor units in humans are sometimes recruited with a quite robust delay (which may exceed 10 s) followed by a firing acceleration and a gradation of muscle force (Desmedt and Godaux, 1975; Kiehn and Eken, 1997). Thus, Kv1.2 channels may be useful in generating smooth control of the onset of muscle output by helping motoneurons to reach their "preferred firing range" (Kiehn and Eken, 1997). Finally, in behavioral contexts that involve a phasic recruitment of motoneurons such as during motor reflexes, the fast activation of Kv1.2 channels may serve as a low-pass filter, allowing motoneurons to respond preferentially to synchronous large-amplitude inputs while filtering out the small ones. Such circumstance may occur when large inputs from spindle primary afferents depolarize motoneurons to trigger a stretch reflex.

To conclude, in addition to mediating the nonlinear spiking properties that are markers of bistable motoneurons, we suggest that Kv1.2 channels play a fundamental role in the dynamics of locomotor circuits by switching motoneurons between gating and amplifying modes.

EXPERIMENTAL PROCEDURES

Further details and an outline of resources used in this work can be found in the Supplemental Experimental Procedures.

Animals

Neonatal (3–11 days old) Wistar rats and adult mice (18 B6SJL, 12 C57BL/6, 45–180 days old) were housed under a 12-hr light/dark cycle in a temperature-controlled area with *ad libitum* access to water and food. All animal care and use conformed to the French regulations (Décret 2010-118) and were approved by the INT Marseille ethics committee CEEA 71 (authorization Nb A9 01 13) for the rat experiments and by Paris Descartes University ethics committee (authorizations CEEA34.MM.064.12 and 01256.02) for the mice experiments.

In Vitro Models

Slice preparation and whole spinal cord preparation were used for the whole-cell recordings and fictive locomotion experiments, respectively. Preparation procedures are detailed in the Supplemental Experimental Procedures.

In Vivo Model

Anesthetized *in vivo* preparations were used for lumbar motoneuron recordings in adult mice. Preparation procedures are detailed in the Supplemental Experimental Procedures.

Intracellular Recordings

From *in vitro* experiments, whole-cell patch-clamp recordings were made from L4-L5 ventrolateral lumbar motoneurons. From *in vivo* experiments, intracellular recordings from lumbar motoneurons were performed with sharp electrodes. Procedures of intracellular recordings are detailed in the Supplemental Experimental Procedures.

Extracellular Recordings

Motor outputs were recorded using extracellular stainless steel electrodes placed in contact with right and left lumbar L5 ventral roots in response to spinal caudal equina stimulation via a suction electrode. See the Supplemental Experimental Procedures for more details.

Simulations

Simulations were performed in the NEURON simulation environment on a multi-compartmental motoneuron model. See the Supplemental Experimental Procedures for more details.

Immunohistochemistry

Transverse spinal cord sections at the lumbar L4-L5 level were processed for immunohistochemistry using antibodies against Ankyrin G, Kv1.1, Kv1.2 channel isoforms. Tissue processing and staining are detailed in the Supplemental Experimental Procedures.

Statistical Analysis

The sample size was estimated considering the variation and mean of the samples. No statistical method was used to predetermine sample size. We used a nonparametric Mann-Whitney test or a Wilcoxon matched pairs test when two groups were compared, and a one-way ANOVA with or without repeated measures for multiple-group comparisons (GraphPad Prism 5 software). For all statistical analyses, the data met the assumptions of the test, and the variance between the statistically compared groups was similar. p values <0.05 were considered significant. As mentioned in the figure legends, all data are presented as mean ± SEM.

SUPPLEMENTAL INFORMATION

Supplemental Information includes Supplemental Experimental Procedures, seven figures, and two tables and can be found with this article online at https://doi.org/10.1016/j.celrep.2018.02.093.

ACKNOWLEDGMENTS

This paper is dedicated to Laurent Vinay, a great scientist who sadly passed away while this research was in progress. He was strongly involved in the initiation of this collaborative project. We are grateful to B. Drouillas and M. Bouhadfane for their assistance in some electrophysiological experiments. We also thank the lab members for their critical reading of this manuscript. This research was financed by a grant from Agence National de la Recherche Scientifique (RhythmDev, ANR-12-BSV4-0011 and CalpaSCI, ANR-16-CE16-0004), the French Institut pour la Recherche sur la Moelle épinière et l'Encéphale (to F.B.), and NIH grant NS17323 (to R.M.H.-W.).

AUTHOR CONTRIBUTIONS

R.B. designed, performed, and analyzed *in vitro* experiments. R.M.H.-W. designed and performed some of the *in vitro* experiments. C.B. designed and performed the immunohistochemistry. L.D. and S.K. co-designed the cell model and performed the analysis. M.M. and D.Z. co-designed and performed *in vivo* experiments. F.B. designed and supervised the whole project, and performed and analyzed some *in vitro* electrophysiological experiments. R.B. and F.B. wrote the manuscript.

DECLARATION OF INTERESTS

The authors declare no competing interests.

Received: November 22, 2017
Revised: February 2, 2018
Accepted: February 23, 2018
Published: March 20, 2018

REFERENCES

Bennett, D.J., Hultborn, H., Fedirchuk, B., and Gorassini, M. (1998a). Short-term plasticity in hindlimb motoneurons of decerebrate cats. J. Neurophysiol. *80*, 2038–2045.

Bennett, D.J., Hultborn, H., Fedirchuk, B., and Gorassini, M. (1998b). Synaptic activation of plateaus in hindlimb motoneurons of decerebrate cats. J. Neurophysiol. *80*, 2023–2037.

Bennett, D.J., Li, Y., and Siu, M. (2001). Plateau potentials in sacrocaudal motoneurons of chronic spinal rats, recorded in vitro. J. Neurophysiol. *86*, 1955–1971.

Bouhadfane, M., Tazerart, S., Moqrich, A., Vinay, L., and Brocard, F. (2013). Sodium-mediated plateau potentials in lumbar motoneurons of neonatal rats. J. Neurosci. *33*, 15626–15641.

Brocard, F., Shevtsova, N.A., Bouhadfane, M., Tazerart, S., Heinemann, U., Rybak, I.A., and Vinay, L. (2013). Activity-dependent changes in extracellular Ca2+ and K+ reveal pacemakers in the spinal locomotor-related network. Neuron *77*, 1047–1054.

Brownstone, R.M. (2006). Beginning at the end: repetitive firing properties in the final common pathway. Prog. Neurobiol. *78*, 156–172.

Brownstone, R.M., Gossard, J.P., and Hultborn, H. (1994). Voltage-dependent excitation of motoneurones from spinal locomotor centres in the cat. Exp. Brain Res. *102*, 34–44.

Carp, J.S., Tennissen, A.M., Mongeluzi, D.L., Dudek, C.J., Chen, X.Y., and Wolpaw, J.R. (2008). An in vitro protocol for recording from spinal motoneurons of adult rats. J. Neurophysiol. *100*, 474–481.

Coetzee, W.A., Amarillo, Y., Chiu, J., Chow, A., Lau, D., McCormack, T., Moreno, H., Nadal, M.S., Ozaita, A., Pountney, D., et al. (1999). Molecular diversity of K+ channels. Ann. N Y Acad. Sci. *868*, 233–285.

Collins, D.F., Burke, D., and Gandevia, S.C. (2002). Sustained contractions produced by plateau-like behaviour in human motoneurones. J. Physiol. *538*, 289–301.

Conway, B.A., Hultborn, H., Kiehn, O., and Mintz, I. (1988). Plateau potentials in alpha-motoneurones induced by intravenous injection of L-dopa and clonidine in the spinal cat. J. Physiol. *405*, 369–384.

Desmedt, J.E., and Godaux, E. (1975). Vibration-induced discharge patterns of single motor units in the masseter muscle in man. J. Physiol. *253*, 429–442.

Duflocq, A., Chareyre, F., Giovannini, M., Couraud, F., and Davenne, M. (2011). Characterization of the axon initial segment (AIS) of motor neurons and identification of a para-AIS and a juxtapara-AIS, organized by protein 4.1B. BMC Biol. *9*, 66.

Durand, J., Filipchuk, A., Pambo-Pambo, A., Amendola, J., Borisovna Kulagina, I., and Guéritaud, J.P. (2015). Developing electrical properties of postnatal mouse lumbar motoneurons. Front. Cell. Neurosci. *9*, 349.

Eken, T., Elder, G.C., and Lømo, T. (2008). Development of tonic firing behavior in rat soleus muscle. J. Neurophysiol. *99*, 1899–1905.

Escoubas, P., Diochot, S., Célérier, M.L., Nakajima, T., and Lazdunski, M. (2002). Novel tarantula toxins for subtypes of voltage-dependent potassium channels in the Kv2 and Kv4 subfamilies. Mol. Pharmacol. *62*, 48–57.

Fowler, S.J., and Kellogg, C. (1975). Ontogeny of thermoregulatory mechanisms in the rat. J. Comp. Physiol. Psychol. *89*, 738–746.

Gao, B.X., and Ziskind-Conhaim, L. (1998). Development of ionic currents underlying changes in action potential waveforms in rat spinal motoneurons. J. Neurophysiol. *80*, 3047–3061.

Gerasimenko, Y., Gorodnichev, R., Puhov, A., Moshonkina, T., Savochin, A., Selionov, V., Roy, R.R., Lu, D.C., and Edgerton, V.R. (2015). Initiation and modulation of locomotor circuitry output with multisite transcutaneous electrical stimulation of the spinal cord in noninjured humans. J. Neurophysiol. *113*, 834–842.

Gorassini, M.A., Bennett, D.J., and Yang, J.F. (1998). Self-sustained firing of human motor units. Neurosci. Lett. *247*, 13–16.

Gorassini, M., Bennett, D.J., Kiehn, O., Eken, T., and Hultborn, H. (1999). Activation patterns of hindlimb motor units in the awake rat and their relation to motoneuron intrinsic properties. J. Neurophysiol. *82*, 709–717.

Gorassini, M., Yang, J.F., Siu, M., and Bennett, D.J. (2002). Intrinsic activation of human motoneurons: reduction of motor unit recruitment thresholds by repeated contractions. J. Neurophysiol. *87*, 1859–1866.

Grissmer, S., Nguyen, A.N., Aiyar, J., Hanson, D.C., Mather, R.J., Gutman, G.A., Karmilowicz, M.J., Auperin, D.D., and Chandy, K.G. (1994). Pharmacological characterization of five cloned voltage-gated K+ channels, types Kv1.1, 1.2, 1.3, 1.5, and 3.1, stably expressed in mammalian cell lines. Mol. Pharmacol. *45*, 1227–1234.

Heckman, C.J., Johnson, M., Mottram, C., and Schuster, J. (2008). Persistent inward currents in spinal motoneurons and their influence on human motoneuron firing patterns. Neuroscientist *14*, 264–275.

Hornby, T.G., McDonagh, J.C., Reinking, R.M., and Stuart, D.G. (2002). Effects of excitatory modulation on intrinsic properties of turtle motoneurons. J. Neurophysiol. *88*, 86–97.

Hornby, T.G., Rymer, W.Z., Benz, E.N., and Schmit, B.D. (2003). Windup of flexion reflexes in chronic human spinal cord injury: a marker for neuronal plateau potentials? J. Neurophysiol. *89*, 416–426.

Hounsgaard, J., and Kiehn, O. (1989). Serotonin-induced bistability of turtle motoneurones caused by a nifedipine-sensitive calcium plateau potential. J. Physiol. *414*, 265–282.

Hounsgaard, J., and Mintz, I. (1988). Calcium conductance and firing properties of spinal motoneurones in the turtle. J. Physiol. *398*, 591–603.

Hounsgaard, J., Hultborn, H., Jespersen, B., and Kiehn, O. (1984). Intrinsic membrane properties causing a bistable behaviour of alpha-motoneurones. Exp. Brain Res. *55*, 391–394.

Hsiao, C.F., Del Negro, C.A., Trueblood, P.R., and Chandler, S.H. (1998). Ionic basis for serotonin-induced bistable membrane properties in guinea pig trigeminal motoneurons. J. Neurophysiol. *79*, 2847–2856.

Hultborn, H., Zhang, M., and Meehan, C.F. (2013). Control and role of plateau potential properties in the spinal cord. Curr. Pharm. Des. *19*, 4357–4370.

Iglesias, C., Meunier, C., Manuel, M., Timofeeva, Y., Delestrée, N., and Zytnicki, D. (2011). Mixed mode oscillations in mouse spinal motoneurons arise from a low excitability state. J. Neurosci. *31*, 5829–5840.

Jell, R.M., Elliott, C., and Jordan, L.M. (1985). Initiation of locomotion from the mesencephalic locomotor region: effects of selective brainstem lesions. Brain Res. *328*, 121–128.

Jiang, Z., Rempel, J., Li, J., Sawchuk, M.A., Carlin, K.P., and Brownstone, R.M. (1999). Development of L-type calcium channels and a nifedipine-sensitive motor activity in the postnatal mouse spinal cord. Eur. J. Neurosci. *11*, 3481–3487.

Jones, H.C., and Keep, R.F. (1988). Brain fluid calcium concentration and response to acute hypercalcaemia during development in the rat. J. Physiol. *402*, 579–593.

Kiehn, O., and Eken, T. (1997). Prolonged firing in motor units: evidence of plateau potentials in human motoneurons? J. Neurophysiol. *78*, 3061–3068.

Kiehn, O., and Harris-Warrick, R.M. (1992). Serotonergic stretch receptors induce plateau properties in a crustacean motor neuron by a dual-conductance mechanism. J. Neurophysiol. *68*, 485–495.

Leroy, F., Lamotte d'Incamps, B., Imhoff-Manuel, R.D., and Zytnicki, D. (2014). Early intrinsic hyperexcitability does not contribute to motoneuron degeneration in amyotrophic lateral sclerosis. eLife *3*, e04046.

Leroy, F., Lamotte d'Incamps, B., and Zytnicki, D. (2015). Potassium currents dynamically set the recruitment and firing properties of F-type motoneurons in neonatal mice. J. Neurophysiol. *114*, 1963–1973.

Li, X.T., Li, X.Q., Hu, X.M., and Qiu, X.Y. (2015). The inhibitory effects of Ca2+ channel blocker nifedipine on rat Kv2.1 potassium channels. PLoS ONE *10*, e0124602.

Miles, G.B., Dai, Y., and Brownstone, R.M. (2005). Mechanisms underlying the early phase of spike frequency adaptation in mouse spinal motoneurones. J. Physiol. *566*, 519–532.

Muennich, E.A., and Fyffe, R.E. (2004). Focal aggregation of voltage-gated, Kv2.1 subunit-containing, potassium channels at synaptic sites in rat spinal motoneurones. J. Physiol. *554*, 673–685.

Nickolls, P., Collins, D.F., Gorman, R.B., Burke, D., and Gandevia, S.C. (2004). Forces consistent with plateau-like behaviour of spinal neurons evoked in patients with spinal cord injuries. Brain *127*, 660–670.

Nisenbaum, E.S., Xu, Z.C., and Wilson, C.J. (1994). Contribution of a slowly inactivating potassium current to the transition to firing of neostriatal spiny projection neurons. J. Neurophysiol. *71*, 1174–1189.

Nishimura, Y., Schwindt, P.C., and Crill, W.E. (1989). Electrical properties of facial motoneurons in brainstem slices from guinea pig. Brain Res. *502*, 127–142.

Pambo-Pambo, A., Durand, J., and Gueritaud, J.P. (2009). Early excitability changes in lumbar motoneurons of transgenic SOD1G85R and SOD1G(93A-Low) mice. J. Neurophysiol. *102*, 3627–3642.

Rasband, M.N., and Trimmer, J.S. (2001). Subunit composition and novel localization of K+ channels in spinal cord. J. Comp. Neurol. *429*, 166–176.

Robertson, B., Owen, D., Stow, J., Butler, C., and Newland, C. (1996). Novel effects of dendrotoxin homologues on subtypes of mammalian Kv1 potassium channels expressed in Xenopus oocytes. FEBS Lett. *383*, 26–30.

Romaiguère, P., Vedel, J.P., and Pagni, S. (1993). Effects of tonic vibration reflex on motor unit recruitment in human wrist extensor muscles. Brain Res. *602*, 32–40.

Russell, S.N., Publicover, N.G., Hart, P.J., Carl, A., Hume, J.R., Sanders, K.M., and Horowitz, B. (1994). Block by 4-aminopyridine of a Kv1.2 delayed rectifier K+ current expressed in Xenopus oocytes. J. Physiol. *481*, 571–584.

Russier, M., Carlier, E., Ankri, N., Fronzaroli, L., and Debanne, D. (2003). A-, T-, and H-type currents shape intrinsic firing of developing rat abducens motoneurons. J. Physiol. *549*, 21–36.

Schwindt, P.C., and Crill, W.E. (1980). Properties of a persistent inward current in normal and TEA-injected motoneurons. J. Neurophysiol. *43*, 1700–1724.

Schwindt, P.C., and Crill, W.E. (1981). Differential effects of TEA and cations on outward ionic currents of cat motoneurons. J. Neurophysiol. *46*, 1–16.

Storm, J.F. (1988). Temporal integration by a slowly inactivating K+ current in hippocampal neurons. Nature *336*, 379–381.

Suzuki, S., Hayami, A., Suzuki, M., Watanabe, S., and Hutton, R.S. (1990). Reductions in recruitment force thresholds in human single motor units by successive voluntary contractions. Exp. Brain Res. *82*, 227–230.

Svirskis, G., and Hounsgaard, J. (1997). Depolarization-induced facilitation of a plateau-generating current in ventral horn neurons in the turtle spinal cord. J. Neurophysiol. *78*, 1740–1742.

Syrbe, S., Hedrich, U.B.S., Riesch, E., Djémié, T., Müller, S., Møller, R.S., Maher, B., Hernandez-Hernandez, L., Synofzik, M., Caglayan, H.S., et al.; EuroEPINOMICS RES Consortium (2015). De novo loss- or gain-of-function mutations in KCNA2 cause epileptic encephalopathy. Nat. Genet. *47*, 393–399.

Takahashi, T. (1990). Membrane currents in visually identified motoneurones of neonatal rat spinal cord. J. Physiol. *423*, 27–46.

Werkman, T.R., Gustafson, T.A., Rogowski, R.S., Blaustein, M.P., and Rogawski, M.A. (1993). Tityustoxin-K alpha, a structurally novel and highly potent K+ channel peptide toxin, interacts with the alpha-dendrotoxin binding site on the cloned Kv1.2 K+ channel. Mol. Pharmacol. *44*, 430–436.

Xie, G., Harrison, J., Clapcote, S.J., Huang, Y., Zhang, J.Y., Wang, L.Y., and Roder, J.C. (2010). A new Kv1.2 channelopathy underlying cerebellar ataxia. J. Biol. Chem. *285*, 32160–32173.